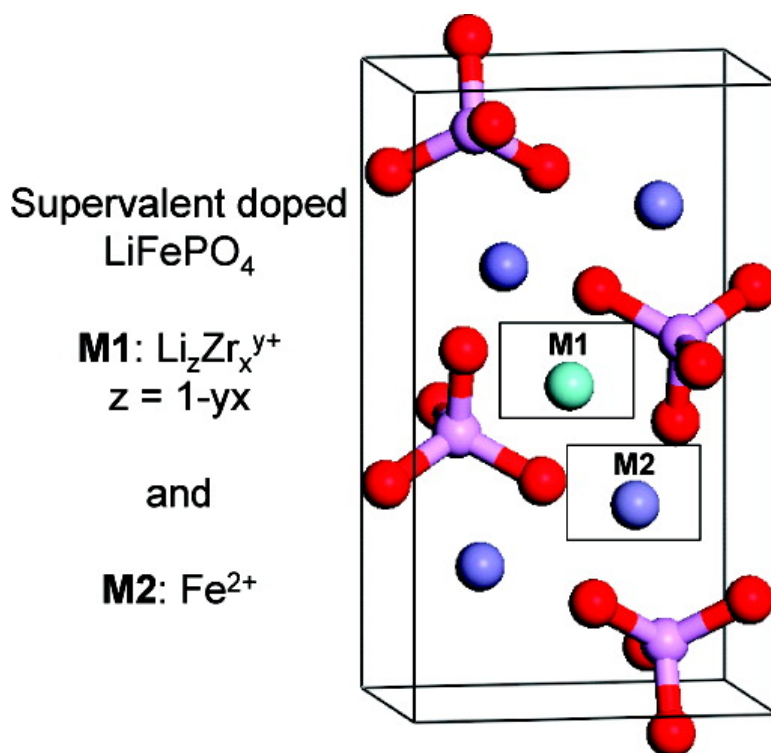


Proof of Supervalent Doping in Olivine LiFePO₄

Marnix Wagemaker, Brian L. Ellis, Dirk Lu#tzenkirchen-Hecht, Fokko M. Mulder, and Linda F. Nazar

Chem. Mater., **2008**, 20 (20), 6313-6315 • DOI: 10.1021/cm801781k • Publication Date (Web): 24 September 2008Downloaded from <http://pubs.acs.org> on November 28, 2008

More About This Article

Additional resources and features associated with this article are available within the HTML version:

- Supporting Information
- Access to high resolution figures
- Links to articles and content related to this article
- Copyright permission to reproduce figures and/or text from this article

[View the Full Text HTML](#)

ACS Publications
High quality. High impact.

Proof of Supervalent Doping in Olivine LiFePO₄

Marnix Wagemaker,^{*,†} Brian L. Ellis,[‡]
Dirk Lützenkirchen-Hecht,[§] Fokko M. Mulder,[†] and
Linda F. Nazar[‡]

Department of Radiation, Radionuclides and Reactors, Faculty of Applied Sciences, Delft University of Technology, Mekelweg 15, 2629 JB Delft, The Netherlands, Department of Chemistry, University of Waterloo, 200 University Avenue West, Waterloo, Ontario, Canada N2L 3G1, and Fachbereich C - Physik, Bergische Universität Wuppertal, Gausstrasse 20, 42097 Wuppertal, Germany

Following the first report of LiFePO₄ as an attractive electrode material for Li-ion batteries,¹ almost a thousand papers to date have been devoted to the understanding and improvement of conductivity in this small-polaron hopping semiconductor. These have encompassed approaches involving surface conductive phases,^{2,3} modification of crystallite size,⁴ and elegant fundamental mechanistic and modeling studies.^{5–7} One early report that spawned much activity suggested that the poor electronic conductivity could be raised by 8 orders of magnitude by supervalent-cation doping, which was proposed to stabilize minority Fe³⁺ hole carriers in the lattice.⁸ The dramatic increase in conductivity was later implicated to be instead partly the result of carbon,⁹ and also metallic iron phosphides/carbophosphides on the LiFePO₄ surface arising from solid-state reactivity at the elevated temperatures used in processing.¹⁰ Although it was shown that both doped and undoped phosphates gave rise to these conductive species and similar conductivity (thus apparently ruling out the contribution of the dopants), their presence within the lattice and their role in electrochemical enhancement still has not been ascertained and remains controversial. Supervalent-cation doping in the bulk material was initially doubted based on the instability of the nonstoichiometric compound.⁹ Other reports indicate that substantial nonstoichiometry can be stabilized in Li_{1–3x}Fe_xMPO₄ olivines (M = Mg, Ni).^{11,12} More recently, the observation

of significant solid solution ranges in LiFePO₄ nanocrystallites less than 170 nm,^{13–15} (likely a general phenomenon related to the particle size),¹⁶ also implies that some level of nonstoichiometry can be sustained in metastable materials prepared by electrochemical delithiation. Regarding dopants, calculations have indicated that aliovalent substitution in the olivine lattice is energetically unlikely.¹⁷ To add to the complexity, recent reports suggest the dopants exist in materials prepared at 600 °C but “exsolve” from the lattice at temperatures above 700 °C, which is the processing temperature that results in enhanced conductivity.¹⁸

We wished to pinpoint the possible dopant location and the material composition in order to shed light on any role that it might play in the electronic and ionic conduction. Previous examination using XRD alone were inconclusive.¹⁹ Here, we report our combined neutron and X-ray diffraction studies which conclusively locate the supervalent-cation dopants (Zr, Nb, Cr) in LiFePO₄. Because neutrons are relatively sensitive to Li and provide large contrast between Li and the dopants, and because X-rays provide good contrast between Fe and the dopants, their combination allows accurate determination of lithium vacancy concentrations, and M1 (Li-site) and M2 (Fe-site) dopant occupations. The results show that low levels of dopants are indeed soluble in the olivine lattice up to the extent of 3 mol % (in bulk materials). They are primarily located on the Li site, thus blocking the Li-ion diffusion in the channels. The aliovalent charge of the dopant is counterbalanced by lithium vacancies. This leads to an overall charge on the iron site of +2.00, and hence no effect on the electronic conductivity is expected.

To prepare the samples, stoichiometric amounts of high purity (>99.99%) Li₂CO₃, FeC₂O₄·2H₂O, NH₄H₂PO₄, as well as Zr(OC₃H₇)₄·C₃H₇OH, Nb(OC₂H₅)₅ and Cr(CH₃COO)₃ were ball-milled with acetone for 6–18 h in silicon nitride media. Powders were heated to 350 °C for 10 h in flowing Ar, reground, and heat-treated at 600 °C in the same atmosphere for up to 8 h. Compositions were targeted to two categories: (1) Li_{1–x}D_x^{y+}FePO₄ intended to determine the preferred dopant site (M1 or M2) and to observe the possible presence of Fe⁺ as suggested by Chiang et al.,¹⁸ (2) Li_{1–yx}D_x^{y+}FePO₄ intended to determine the vacancy concentration on the M1 site when Fe is present in the +2 valence state. Neutron diffraction was performed on

* Corresponding author. E-mail: m.wagemaker@tudelft.nl.

† Delft University of Technology.

‡ University of Waterloo.

§ Bergische Universität Wuppertal.

- (1) Padhi, A. K.; Nanjundaswamy, K. S.; Goodenough, J. B. *J. Electrochem. Soc.* **1997**, *144*, 1188.
- (2) Ravet, N. Improved iron based cathode material. In *Proceedings of the Electrochemical Society Fall Meeting*, Honolulu, HI, Oct 1999; Electrochemical Society: Pennington, NJ, 1999; Abstr. No. 127.
- (3) Huang, H.; Yin, S. C.; Nazar, L. F. *Electrochem. Solid-State Lett.* **2001**, *4*, A170.
- (4) Delacourt, C.; Poizot, P.; Levasseur, S.; Masquelier, C. *Electrochem. Solid-State Lett.* **2006**, *9*, A352.
- (5) Zhou, F.; Maxisch, T.; Ceder, G. *Phys. Rev. Lett.* **2006**, *97*.
- (6) Morgan, D.; Van der Ven, A.; Ceder, G. *Electrochem. Solid-State Lett.* **2004**, *7*, A30.
- (7) Srinivasan, V.; Newman, J. *J. Electrochem. Soc.* **2004**, *151*, A1517.
- (8) Chung, S. Y.; Bloking, J. T.; Chiang, Y. M. *Nat. Mater.* **2002**, *1*, 123.
- (9) Ravet, N.; Abouimrane, A.; Armand, M. *Nat. Mater.* **2003**, *2*, 702.
- (10) Herle, P. S.; Ellis, B.; Coombs, N.; Nazar, L. F. *Nat. Mater.* **2004**, *3*, 147.
- (11) Goni, A.; Lezama, L.; Arriortua, M. I.; Barberis, G. E.; Rojo, T. *J. Mater. Chem.* **2000**, *10*, 423.

- (12) Goni, A.; Lezama, L.; Pujana, A.; Arriortua, M. I.; Rojo, T. *Int. J. Inorg. Mater.* **2001**, *3*, 937.
- (13) Yamada, A.; Takei, Y.; Koizumi, H.; Sonoyama, N.; Kanno, R.; Itoh, K.; Yonemura, M.; Kamiyama, T. *Chem. Mater.* **2006**, *18*, 804.
- (14) Meethong, N.; Huang, H. Y. S.; Carter, W. C.; Chiang, Y. M. *Electrochem. Solid-State Lett.* **2007**, *10*, A134.
- (15) Meethong, N.; Huang, H. Y. S.; Speakman, S. A.; Carter, W. C.; Chiang, Y. M. *Adv. Funct. Mater.* **2007**, *17*, 1115.
- (16) Wagemaker, M.; Borghols, W. J. H.; Eck, E. R. H.; Kentgens, A. P. M.; Kearley, G. J.; Mulder, F. M. *Chem.—Eur. J.* **2007**, *13*, 2023.
- (17) Islam, M. S.; Driscoll, D. J.; Fisher, C. A. J.; Slater, P. R. *Chem. Mater.* **2005**, *17*, 5085.
- (18) Chiang, Y. M. Conductive Lithium Storage Electrode. U.S. patent 7338734, 2008.
- (19) Ellis, B.; Herle, P. S.; Rho, Y. H.; Nazar, L. F.; Dunlap, R.; Perry, L. K.; Ryan, D. H. *Faraday Discuss.* **2007**, *134*, 119.

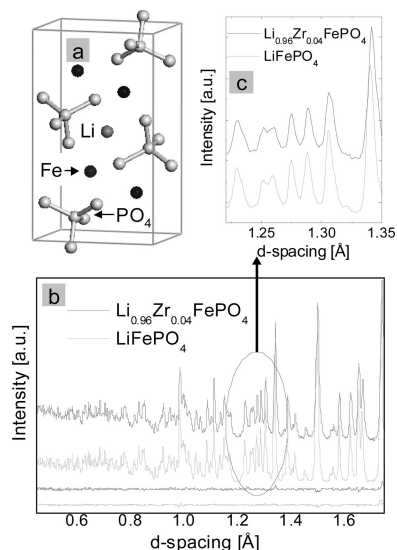


Figure 1. (a) LiFePO_4 $Pnma$ unit cell with the split Li-ion (medium gray) position in the center. (b) Neutron diffraction data for LiFePO_4 and $\text{Li}_{0.96}\text{Zr}_{0.04}\text{FePO}_4$ (target composition) including the difference between the fits and data. The fit residues are $wR_p = 1.7\%$, $R_p = 1.9\%$ and $wR_p = 1.7\%$, $R_p = 1.8\%$, respectively. (c) The same data as in (b) shown for a limited d -spacing range.

GEM, the time-of-flight neutron diffraction instrument at ISIS (Rutherford Appleton Laboratories, Didcot, UK), and these data were refined simultaneously with X-ray diffraction data collected on an X-pert pro mpd, Philips/Panalytical) using X-ray radiation from a Cu-anode ($0.4 \times 12 \text{ mm}^2$ line focus, 45 kV, 40 mA). Details of the fitting procedure can be found in the Supporting Information.

Fitting the undoped LiFePO_4 material, unit cell shown in Figure 1a, using anisotropic temperature factors leads to the exact site occupancies predicted by stoichiometry (see the Supporting Information), unlike materials prepared by hydrothermal synthesis at low temperatures (130 °C), which can exhibit Li/Fe site mixing.^{20,21}

Figure 1b compares the neutron diffraction patterns of undoped LiFePO_4 and one of the doped materials, $\text{Li}_{0.96}\text{Zr}_{0.04}\text{FePO}_4$. Careful inspection of the patterns reveals several subtle but significant differences between the two patterns. Most apparent is a shift in the position of the peaks, indicating a small but clear difference in the lattice parameters, and differences in peak intensities indicating a difference in the doped and undoped materials. These are highlighted for a selected region expanded in Figure 1c. Simultaneous fitting of the X-ray and neutron data for $\text{Li}_{0.96}\text{Zr}_{0.04}\text{FePO}_4$ converged with excellent agreement factors ($R_{wp} = 0.023$, $R_{exp} = 0.017$, $\chi^2 = 1.4$), revealing that only close to 0.01Zr is accommodated in the M1 site, not 0.04Zr. A very minute amount of impurity was barely detectable ($\text{LiZr}_2(\text{PO}_4)_3$), explaining the discrepancy between the target and actual composition. Attempts to place Zr on the M2 site also resulted in much poorer agreement factors. However, fitting the M2 site with a partial occupation of Li (keeping the atomic occupation on M2 = 1.00) yielded the final refined

Table 1. Dopant Concentrations, The Fe Valence and Average M1–O Bond Distances Resulting from Simultaneous Refinement of the X-ray and Neutron Data for the Samples with Composition $\text{Li}_{1-x}\text{D}_x\text{FePO}_4$, $D = \text{Zr}$ and Nb, and $\text{Li}_{1-x}\text{D}_x^{\gamma+}\text{FePO}_4$, $D = \text{Zr}$ and Cr

target stoichiometry	M1 and M2 composition [M1][M2]	dopant M1/M2 occupancy ± 0.001	Fe M2 valence ± 0.006	avg M1–O distance (Å) ± 0.002
LiFePO_4	[Li][Fe]		2.000	2.150
$\text{Li}_{1-x}\text{D}_x\text{FePO}_4$ Compositions				
$\text{Li}_{0.99}\text{Zr}_{0.01}\text{A}^a$	$[\text{Li}_{0.979}\text{Zr}_{0.008}][\text{Li}_{0.008}\text{Fe}_{0.992}]$	0.008/0.000	1.998	2.151
$\text{Li}_{0.96}\text{Zr}_{0.04}\text{A}^a$	$[\text{Li}_{0.966}\text{Zr}_{0.009}][\text{Li}_{0.007}\text{Fe}_{0.993}]$	0.009/0.000	2.003	2.153
$\text{Li}_{0.99}\text{Nb}_{0.01}\text{A}^a$	$[\text{Li}_{0.986}\text{Nb}_{0.005}][\text{Li}_{0.007}\text{Fe}_{0.993}]$	0.005/0.000	1.998	2.152
$\text{Li}_{1-x}\text{D}_x^{\gamma+}\text{FePO}_4$ Compositions				
$\text{Li}_{0.96}\text{Zr}_{0.01}\text{A}^a$	$[\text{Li}_{0.976}\text{Zr}_{0.008}][\text{Li}_{0.004}\text{Fe}_{0.996}]$	0.008/0.000	1.996	2.154
$\text{Li}_{0.88}\text{Zr}_{0.03}\text{A}^a$	$[\text{Li}_{0.891}\text{Zr}_{0.022}][\text{Li}_{0.004}\text{Zr}_{0.009}\text{Fe}_{0.987}]$	0.023/0.008	2.005	2.157
$\text{Li}_{0.91}\text{Cr}_{0.03}\text{A}^a$	$[\text{Li}_{0.924}\text{Cr}_{0.021}][\text{Cr}_{0.008}\text{Fe}_{0.992}]$	0.021/0.008	2.004	2.156

^a A = FePO_4

composition of $[\text{Li}_{0.966}\text{Zr}_{0.009}][\text{Li}_{0.007}\text{Fe}_{0.993}]\text{PO}_4$ (Table 1). Thus, a very small amount of Li^+ is accommodated on the Fe site in this case. The formal oxidation state on the iron is thus $+2.003 \pm 0.006$.²² The complete refinement results are summarized in the Supporting Information.

In the $\text{Li}_{0.99}\text{Zr}_{0.01}\text{FePO}_4$ material, refinement resulted in the composition $[\text{Li}_{0.979}\text{Zr}_{0.008}][\text{Li}_{0.008}\text{Fe}_{0.992}]\text{PO}_4$; close to the target. Substituting Nb as the dopant resulted in a similar refinement corresponding to $[\text{Li}_{0.986}\text{Nb}_{0.005}][\text{Li}_{0.007}\text{Fe}_{0.993}]\text{PO}_4$ for the targeted $\text{Li}_{0.99}\text{Nb}_{0.01}\text{FePO}_4$ composition. Thus, in summary for the $\text{Li}_{1-x}\text{D}_x\text{FePO}_4$ materials (Table 1), dopant substitution on the M1 site indeed occurs, but less dopant than targeted appears to be actually soluble in the lattice. The aliovalent charge on the dopant ion is accommodated by M1 site vacancies and an M2 site substitution of Fe^{2+} for Li^+ , to give rise to an overall Fe^{2+} oxidation state as in stoichiometric, undoped LiFePO_4 .

The $\text{Li}_{0.99}\text{Zr}_{0.01}\text{FePO}_4$ sample was further subjected to partial chemical delithiation using 0.2 equivalents of NOBF_4 . The refinement showed a mixture of a Li-rich phase ($\text{Li}_{0.93}\text{Zr}_{0.008}\text{FePO}_4$; $a = 10.3184 \text{ \AA}$; $b = 6.0003 \text{ \AA}$; $c = 4.6950 \text{ \AA}$; $V = 290.684 \text{ \AA}^3$) and a Li-poor phase ($\text{Li}_{0.03}\text{Zr}_{0.008}\text{FePO}_4$). These solubility limits for “ $\text{Li}_{1-\beta}\text{FePO}_4$ ” and “ $\text{Li}_\alpha\text{FePO}_4$ ” ($1 - \beta = 0.93$; $\alpha = 0.03$) indicate a slightly larger miscibility gap than reported by Yamada et al.²³ This is consistent with the slightly larger particle sizes observed here (determined from size broadening, of about 150 nm), compared with that of the previous report of about 100 nm. Recent particle size dependent studies that show the miscibility gap decreases for smaller particles.^{14,24}

To investigate the extent of Li deficiency that compensates for the charge in the doped materials, we prepared compositions of $\text{Li}_{0.96}\text{Zr}_{0.01}\text{FePO}_4$, $\text{Li}_{0.88}\text{Zr}_{0.03}\text{FePO}_4$, and $\text{Li}_{0.91}\text{Cr}_{0.03}\text{FePO}_4$. A summary of the resulting compositions from simultaneous fitting of the X-ray and neutron data is shown in Table 1. For these compositions, the Fe oxidation state again does not differ significantly from +2. The

(22) The error in the iron valence was determined through the error in the atomic occupancies resulting from the Rietveld refinement.

(23) Yamada, A.; Koizumi, H.; Nishimura, S. I.; Sonoyama, N.; Kanno, R.; Yonemura, M.; Nakamura, T.; Kobayashi, Y. *Nat. Mater.* **2006**, *5*, 357.

(24) Wagemaker, M.; Borghols, W. J. H.; Mulder, F. M. *J. Am. Chem. Soc.* **2007**, *129*, 4323.

(20) Chen, J. J.; Whittingham, M. S. *Electrochem. Commun.* **2006**, *8*, 855.

(21) Chen, J. J.; Vacchio, M. J.; Wang, S. J.; Chernova, N.; Zavalij, P. Y.; Whittingham, M. S. *Solid State Ionics* **2008**, *178*, 1676.

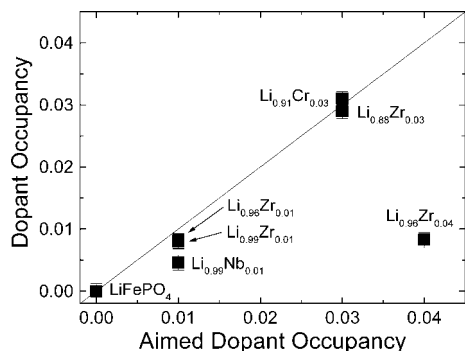


Figure 2. Supervalent doping occupancies from combined X-ray and neutron diffraction refinement plotted versus the targeted dopant concentration.

Table 2. Lattice Parameters for Doped $\text{Li}_{1-x}\text{D}_x\text{FePO}_4$, $D = \text{Zr, Cr, and Nb}$ Compositions

refined stoichiometry	a (Å) ± 0.001	b (Å) ± 0.001	c (Å) ± 0.001	V (Å ³) ± 0.005
LiFePO_4	10.318	6.004	4.694	290.762
(iii) $[\text{Li}_{0.979}\text{Zr}_{0.008}][\text{Li}_{0.008}\text{Fe}_{0.992}]\text{PO}_4$	10.311	6.001	4.695	290.485
(iv) $[\text{Li}_{0.966}\text{Zr}_{0.009}][\text{Li}_{0.007}\text{Fe}_{0.993}]\text{PO}_4$	10.312	5.998	4.697	290.447
(v) $[\text{Li}_{0.986}\text{Nb}_{0.005}][\text{Li}_{0.007}\text{Fe}_{0.993}]\text{PO}_4$	10.321	6.005	4.694	290.911
(i) $[\text{Li}_{0.891}\text{Zr}_{0.022}][\text{Li}_{0.004}\text{Zr}_{0.009}\text{Fe}_{0.987}]\text{PO}_4$	10.324	6.005	4.698	291.255
(ii) $[\text{Li}_{0.924}\text{Cr}_{0.021}][\text{Cr}_{0.08}\text{Fe}_{0.92}]\text{PO}_4$	10.323	6.003	4.696	290.963

intended deficiency of Li permits larger solubility of the dopant in Li deficient materials compared to the $\text{Li}_{1-x}\text{D}_x\text{FePO}_4$ compositions such that the target stoichiometry closely matches the stoichiometry of the fitted data. This is further magnified by a comparison of the intended dopant occupancy versus calculated dopant occupancy resulting from the data fitting as shown in Figure 2. Although both the M1 and the M2 sites were considered, fitting indicates preferred occupation of the dopant on the M1 site in all cases, in agreement with earlier speculations.⁸

The occupation of dopants and vacancies in the lattice can be expected to result in very small changes of the lattice parameters, presented in Table 2. Although full oxidation of LiFePO_4 results in a 6% decrease of the unit cell volume, there is an increase in the size of the vacant M1 octahedron. Compositions such as $\text{Li}_{0.88}\text{Zr}_{0.03}\text{FePO}_4$ (i), or $\text{Li}_{0.91}\text{Cr}_{0.03}\text{FePO}_4$ (ii), which sustain a quantity of M1 site vacancies in excess of 2 mol %, experience a slight increase in unit cell volume. Conversely compositions such as $\text{Li}_{0.99}\text{Zr}_{0.01}\text{FePO}_4$ (iii) or $\text{Li}_{0.96}\text{Zr}_{0.04}\text{FePO}_4$ (iv), which stabilize few vacancies (<2 mol %), tend to give rise to a slight contraction of the unit-cell volume. This may be a consequence of the replacement of Li^+ (radius: 76 pm) with the slightly smaller Zr^{4+} ion (72 pm). The fact that Nb^{5+} (64 pm) substitution results in a larger cell volume suggests there are other subtle factors that may influence this parameter. Indeed, the factors affecting lattice parameters remain poorly understood at present. For example, two previous doped olivine studies that also show high defect concentrations on the M1 site depict contradictory trends: in one case, the unit cell volume contracts (Fe^{3+} -doped LiMgPO_4), and in the other case (Fe^{3+} -doped LiNiPO_4) it expands.^{11,12} The effect of the vacancies on the Li–O tunnel dimension follows the expected trend in the materials studied here: the average M1–O bond distances for LiFePO_4 , “ $\text{Li}_{0.96}\text{Zr}_{0.04}\text{FePO}_4$ ” and

“ $\text{Li}_{0.88}\text{Zr}_{0.03}\text{FePO}_4$ ” are 2.150 Å; 2.153 Å; 2.157 Å (respectively), as calculated from the refined bond length data. Increased vacancy concentration can be expected to lead to longer Li–O distances due to increased O–O repulsion in the empty sites. Nonetheless, the effect is extremely small, especially given our estimated error in the refinement methods.

We noted above that the refinement results for all of the present doped $\text{Li}_{1-x}\text{D}_x\text{FePO}_4$ – and including the $\text{Li}_{1-x}\text{D}_x\text{FePO}_4$ materials – do not indicate a detectable amount of Fe^{3+} (within the limits of error), as is demonstrated by the effective Fe valence summarized in Table 1. However, Yamada²³ showed that solid solutions with Li deficiency exist in the undoped material (compositions $\text{Li}_{1-\beta}\text{FePO}_4$ and $\text{Li}_\alpha\text{FePO}_4$, where $1 - \beta = 0.89$ and $\alpha = 0.05$), and where the solubility domain appears to depend on the particle size.^{14,24} Such two phase mixtures should exhibit the same 8 order of magnitude of conductivity increase due to the presence of Fe^{3+} hole carriers in $\text{Li}_{0.89}\text{FePO}_4$ (or Fe^{2+} electron carriers in $\text{Li}_{0.05}\text{FePO}_4$) – which is not observed. This is probably due to the fact that low carrier concentrations in small polaron “hopping” semiconductors have a fundamentally different effect than that in intrinsic semiconductors such as Si.²⁵ Therefore, it is unlikely that Li-deficiencies and/or mixed $\text{Fe}^{2+/3+}$ valence, whether or not created by the dopant, are responsible for the enhanced conductivity.

In conclusion, neutron and X-ray diffraction of aliovalent cation doped LiFePO_4 ($\text{Li}_{1-x}\text{D}_x\text{FePO}_4$; $D = \text{Zr, Nb, Cr}$) is used to show that supervalent-cation doping up to ~3% atomic substitution can be hosted in the LiFePO_4 lattice in bulk materials prepared by a solid state route at 600 °C. The results clearly show that the dopant resides primarily on the M1 (Li) site. Samples of the type $\text{Li}_{1-x}\text{D}_x\text{FePO}_4$ typically showed refined dopant concentrations lower than intended. Precise refinement also showed that the aliovalent dopant charge was balanced by lithium vacancies, with the total charge on the iron site being +2.000 (± 0.006), within the limit of experimental error, not indicating enhanced electronic conductivity due to the dopant. Furthermore, the dopant causes only a 0.3% increase in the size of the lithium channels, which is not expected to influence the Li-ion mobility. Rather, the location of the immobile high valent dopant within the lithium channels may hinder Li ion diffusion.

Acknowledgment. We thank Winfried Kockelmann for assistance with the neutron diffraction experiments at GEM (ISIS).

Supporting Information Available: The detailed fit procedure, tables of crystal data with refined atomic coordinates and occupancies for target compositions LiFePO_4 , $\text{Li}_{0.96}\text{Zr}_{0.04}\text{FePO}_4$ (iv), and $\text{Li}_{0.88}\text{Zr}_{0.03}\text{FePO}_4$ (i) together with their Rietveld refinements (PDF); crystallographic files for these compositions (CIF). This material is available free of charge via the Internet at <http://pubs.acs.org>. CM801781K